



Removal of Alizarin Red and Purpurin from Aqueous Solutions Using Fe_3O_4 Magnetic Nanoparticles

Ghodratollah Absalan^{a,*}, Asma Bananejad^a and Maryam Ghaemi^b

^aProfessor Massoumi Laboratory, Department of Chemistry, Faculty of Sciences, Shiraz University, Shiraz 71454, Iran

^bDepartment of Marine Science, Iranian National Institute for Oceanography and Atmospheric Science, No. 3, Etemadzadeh St., Fatemi Ave., Tehran, 1411813389, IR Iran

(Received 15 May 2016, Accepted 10 November 2016)

The applicability of Fe_3O_4 nanoparticles (Fe_3O_4 NPs) for removing alizarin and purpurin from aqueous solutions has been reported. The influence of nanoparticle dosage, pH of the sample solution, individual dye concentration, contact time between the sample and the adsorbent, temperature, and ionic strength of the sample solution were studied by performing a batch adsorption technique. The maximum removal of 5-100 mg l⁻¹ of individual dyes from an aqueous sample solution at pH 5.0 was achieved within 5.0 min when an adsorbent amount of 20 mg was used. The kinetic results revealed that the pseudo-second-order equation is the best model to analyze the adsorption mechanism. The isotherm analysis indicated that the equilibrium data are well fitted to the Langmuir isotherm model with maximum adsorption capacities of 45.87 and 40.48 mg g⁻¹ of the adsorbent for removal of alizarin and purpurin, respectively. According to the experimental results, about 99% of alizarin and 95% of purpurin were removed from aqueous solutions under applying the optimal experimental conditions.

Keywords: Iron oxide magnetic nanoparticles, Alizarin red, Purpurin, Dye removal, Anthraquinone dyes

INTRODUCTION

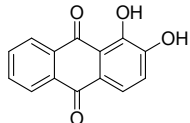
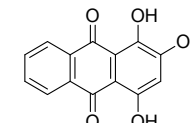
Dyes, the most visible pollutants, are presented in the effluents discharged from various industries: textile, dyeing, leather, food processing, paper, and dye manufacturing. Considerable amounts of synthetic dyes are lost to wastewater during textile processing that is quite undesirable [1,2]. Because of their synthetic natures and complex aromatic molecular structures, dyes are almost non-biodegradable in the ecosystem [3]. The importance of the potential pollution of dyes and their intermediates has been incited with the toxic nature of many dyes, different mutagenic effects, skin diseases and skin irritation and allergies. Moreover, they are dangerous because their microbial degradation compounds, such as benzidine or other aromatic compounds have carcinogenic effect [1,3,

4].

Alizarin red (1,2-dihydroxy-9,10-anthraquinone) and purpurin (1,2,4-trihidroxy anthraquinone), Table 1, are natural dyes obtained from madder (*Rubia tinctorum L.*, Rubiaceae) [5]. They have been used in textile industry since early antiquity because they contain hydroxyl groups that make them soluble in water with great affinity toward silk and wool without aiding auxiliary binding agents [6]. Anthraquinone dyes like alizarin and purpurin are recalcitrant and durable pollutants, released especially by textile industries in the aquatic ecosystems [7]. For these reasons, both dyes have been chosen as target pollutants in many research fields considering dye treatment [8-10]. For instance, Panizza and Cerisola [11] investigated the degradation of alizarin red by electro-Fenton process using an O₂-fed carbon polytetrafluoroethylene cathode. They showed that alizarin red is completely oxidized within 4.0 h of electrolysis. Dabiri *et al.* studied a microwave-assisted

*Corresponding author. E-mail: absalan@susc.ac.ir

Table 1. Some Characteristics of the Investigated Dyes

Characteristic	Alizarin red		Purpurin		
Molecular formula	$C_{14}H_8O_4$			$C_{14}H_8O_5$	
Chemical name	1,2-Dihydroxy-9,10-anthraquinone			1,2,4-Trihydroxyanthracene-9, 10-dione	
Molecular weight	240.20 ($g\ mol^{-1}$)			256.21 ($g\ mol^{-1}$)	
λ_{max}	420 (nm)			470 (nm)	
Class	Anthraquinone			Anthraquinone	
Acidity constants	pK_{a_1}	pK_{a_2}	pK_{a_1}	pK_{a_2}	pK_{a_3}
	5.25	11.50	5.18	7.65	10.27
Chemical structure					

extraction (MAE) procedure for alizarin and purpurin. Their results showed that the separation and quantitative determination of the dyes could be carried out in a short period of time by a developed high-performance liquid chromatographic method equipped with a UV detection system [13].

Adsorption on solid materials is an effective separation technique due to its low cost, ease of operation without harmful residues, simplicity of the design and possibility of the adsorbent regeneration [14]. Hence, it has been extensively used for removal of different chemicals from aqueous solutions [15-17]. The efficient applicability of an adsorption process mainly depends on the physical and chemical characteristics of the adsorbent, which is expected to have high adsorption capacity and to be recoverable and available at economical cost. Currently, various potential adsorbents have been implemented for removal of specific organics from water samples. In this regard, magnetic nanoparticles (MNPs) have been studied extensively as novel adsorbents with large surface area, high adsorption capacity and small diffusion resistance. For instance, they have been used for separation of chemical species such as environmental pollutants, metals, dyes, and gases [18-21]. Moreover, they make separation easier and faster by being

recovered with an external magnet field without additional centrifugation or filtration process [22]. For example, by using chitosan coating on the surface of magnetite Fe_3O_4 , Fan *et al.* synthesized an adsorbent as a template for adsorption and removal of alizarin red from aqueous solutions [12].

The utilization of solid-phase extraction (SPE) as a preconcentration technique has increasingly progressed because it could effectively handle small samples using only small volumes of organic solvents with simple instrumentation. In this respect, magnetic solid-phase extraction (MSPE) technique is performed on the basis of the adsorption of target analytes from liquid samples using solid adsorbents with magnetic properties. It has many advantages over the conventional SPE including simplicity, high efficiency, low cost, and high selectivity. Moreover, the corresponding procedure does not perform additional steps such as centrifugation, precipitation, or filtration of the sample. Moreover, MSPE can be applied not only for homogeneous solutions but also for liquid suspensions. This is a common benefit of magnetic separation techniques because of the fact that most of accompanying impurities are diamagnetic and do not interfere with magnetic particles during the magnetic separation step [23].

Regarding the chemical structure of Fe_3O_4 nanoparticles, those organic compounds that could complex either Fe^{2+} or Fe^{3+} ions or interact with the negative oxygen sites of the nanoparticles (*e.g.* through H-bonding) at specific controlled experimental conditions such as pH of the sample, temperature, ionic strength, *etc.* could be adsorbed on the surface of these nanoparticles. That is why a lot of research papers have focused on modification of MNPs with different organic compounds in order to extent the applicability of these particles in different fields such as separation sciences. For instance, ionic liquids have been used to improve the selectivity through modifying the surface of the nanoparticles for extraction purposes [19]. However, there are several advantages forecasted for the use of bared magnetic nanoparticles, where dyes are directly adsorbed onto their surfaces. For instance, the absence of coating results in smaller particles, therewith providing higher surface area for adsorption of dyes. In addition, MNPs allow a greater response to the applied magnetic field at this condition making separation easier. Moreover, MNPs can be present as a stable suspension, thereby allowing uniform distribution in a reaction mixture [24].

In this work, the possibility of using Fe_3O_4 nanoparticles as adsorbent for significant removal of alizarin red and purpurin from aqueous solutions has been investigated. The effect of principle factors including pH, contact time between reagents, dosage of MNPs, initial dyes concentration and temperature were studied. The sorption equilibrium and kinetic data were analyzed by means of different models to understand the possible sorption mechanism of the dye molecules onto the magnetic nanoparticles.

EXPERIMENTAL

Chemicals and Reagents

The dyes used in this study, alizarin red and purpurin, were purchased from Merck and Acros, respectively. Sodium hydroxide, hydrochloric acid, $\text{FeCl}_3 \cdot 6\text{H}_2\text{O}$, $\text{FeSO}_4 \cdot 7\text{H}_2\text{O}$, ethanol and dimethyl sulfoxide were purchased from Merck. The stock solutions of alizarin and purpurin were prepared in dimethylsulfoxide. For treatment experiments, the desired concentrations of the dyes were prepared by successive dilution of their stock solutions in

ethanol.

Instrumentation

A UV-Vis spectrophotometer model Pharmacia Ultraspec 4000, equipped with a 1-cm quartz cell was used for recording the visible spectra and absorbance measurements. A transmission electron microscope ((Philips CM 10 TEM) was used for recording the TEM images. The XRD measurements were performed on an XRD Bruker D8 Advance. The FTIR spectra were recorded on a Shimadzu FTIR 8000 spectrometer. A Metrohm 780 pH meter was used for monitoring the pH of the solutions. A water ultrasonicator (Model CD-4800, China) was used to disperse the nanoparticles in aqueous solutions and a super magnet Nd-Fe-B (1.4 T, 10 cm × 5 cm × 2 cm made in China) was used for separation purposes. All measurements were performed at ambient temperature.

Preparation of Fe_3O_4 Nanoparticles

The nanoparticles of Fe_3O_4 were prepared by co-precipitating Fe(II) and Fe(III) ions in sodium hydroxide solution with constant stirring at 1500 rpm as recommended [25]. To do so, equimolar amounts of 0.25 M $\text{FeSO}_4 \cdot 7\text{H}_2\text{O}$ and 0.50 M $\text{FeCl}_3 \cdot 6\text{H}_2\text{O}$ were mixed and the resulted solution was added dropwise to 1.0 M NaOH to obtain the maximum yield for magnetic nanoparticles during the co-precipitation process. The precipitate was washed for three times with 50 ml distilled water in each trial. Nanoparticles and distilled water mixture was dispersed by ultrasonication for a period of 10.0 min at room temperature. The synthesized Fe_3O_4 nanoparticles were magnetically separated [19]. The yield for preparation of the nanoparticles was 90% based on the reproducing the above mentioned procedure.

Dye removal Experiments

To study the effect of important parameters like the nanoparticle dosage, pH of the solution, dye concentration, contact time, ionic strength, and temperature on the adsorptive removal of alizarin and purpurin, batch experiments were conducted. Aliquots of 10 ml of each dye solution with initial concentrations of 5-200 mg l⁻¹ in the pH range of 2.5-12.5 were prepared and transferred into individual beakers. A known dosage of Fe_3O_4 in the range of 10.0-35.0 mg was added to each solution and the

suspension was immediately stirred with a magnetic stirrer for a predefined period of 1.0-20.0 min. After the mixing time elapsed, the Fe_3O_4 nanoparticles were magnetically separated and each solution was analyzed for the residual dye. The percent adsorption of dye, *i.e.* the dye-removal efficiency of Fe_3O_4 was determined by using the following equation:

$$\text{Dye removal efficiency (\%)} = \frac{(C_0 - C_f)}{C_0} \times 100 \quad (1)$$

where C_0 and C_f (in mg l^{-1}) represent the initial and final (after adsorption) dye concentrations, respectively. All experiments were performed at room temperature. It should be mentioned that the values of all parameters reported above are those used during the optimization experiments. The optimum values have been cited in the subsequent sections.

RESULTS AND DISCUSSION

Characterization of the Fe_3O_4 NPs

The transmission electron microscopy (TEM) image for the synthesized nanoparticles indicated narrow distribution with average particle diameter of 10 nm (Fig. 1A). The X-Ray diffraction (XRD) pattern of Fe_3O_4 NPs, shown in Fig. 1B, indicates six characteristic peaks for Fe_3O_4 ($2\theta = 30.1, 35.5, 43.3, 53.4, 57.2$ and 62.5) corresponding to indices (220), (311), (400), (422), (511) and (440). The Fourier transform infrared (FTIR) spectra of Fe_3O_4 nanoparticles are shown in Fig. 2. The broad absorption band at 3440 cm^{-1} indicates the presence of surface hydroxyl groups (O-H stretching) and the bands at low wavenumbers ($\leq 700 \text{ cm}^{-1}$) are related to vibrations of the Fe-O bonds in iron oxide. The presence of magnetic nanoparticles can be proven by appearance of two strong absorption bands around 632 and 585 cm^{-1} [25]. The Fe-O bond peak of the bulk magnetite is observed at 571 cm^{-1} . The pH value at the point of zero charge (pH_{pzc}) of Fe_3O_4 nanoparticle is 6.5 [19].

To confirm the adsorption of dyes on Fe_3O_4 nanoparticles, the FTIR spectra of dyes and nanoparticles after adsorption of individual dyes were compared. In the case of alizarin dye (Fig. 3), peaks at 1312 and 1496 cm^{-1} correspond to benzene ring and peaks at 1668 and 3468 cm^{-1} correspond to keto (C=O) and phenol (-OH) groups attached

to the aromatic rings of the dye molecules, respectively [26]. In the case of alizarin adsorbed onto the Fe_3O_4 nanoparticles compared with free Fe_3O_4 nanoparticle, new peaks are observed in 1308, 1502 and 1670 cm^{-1} showing that alizarin is absorbed on the surface of nanoparticles. Also, the observed shift in the position of these peaks compared with free alizarin may indicate the attachment of dye onto the surface of Fe_3O_4 nanoparticles. Shifts observed for peaks in 586 and 634 cm^{-1} (now at 638 cm^{-1}) may correspond to the attachment of dye onto the Fe_3O_4 surface. In the case of purpurin dye (Fig. 4), peaks at 1338, 1488 cm^{-1} correspond to benzene ring and peaks at 1652 and 3452 cm^{-1} correspond to keto (C=O) and phenol (-OH) groups attached to the aromatic rings of the dye molecules, respectively [27]. In the case of purpurin adsorbed onto the Fe_3O_4 nanoparticle compared to Fe_3O_4 nanoparticle itself, new peaks are observed at 1336 and 1656 cm^{-1} showing that purpurin has been adsorbed on the surface of nanoparticles. Shifts observed at 586 and 634 cm^{-1} (now at 605 and 676 cm^{-1}) may correspond to the attachment of dye onto the Fe_3O_4 surface. These results indicate that the dyes have been adsorbed on the surface of nanoparticles without being degraded.

Effect of Nanoparticle Dosage and Sample Volume

The effect of Fe_3O_4 dosage on removal of alizarin and purpurin was investigated using a batch technique by adding a known quantity of the adsorbent, in the range of 10.0-35.0 mg of its powder form, into individual beakers containing 10 ml of the dye solution. The initial dye concentrations and the pH of the solutions were fixed at 20.0 mg l^{-1} and 5.0, respectively. The resulting suspension was immediately stirred for 5.0 min. After the mixing time elapsed, the Fe_3O_4 nanoparticles were magnetically separated and the solution was analyzed for the residual dye. As shown in Fig. 5, the percent removal of both dyes increased with increasing Fe_3O_4 dosage up to 20.0 mg and reached to over 99% for alizarin and 95% for purpurin at this dosage. This observation can be explained by the availability of a greater number of adsorption sites for dye molecules at greater Fe_3O_4 dosages. Consequently, further increase of the adsorbent dosage did not affect the removal of dye. Hence, the optimum dosage of Fe_3O_4 powder for removing alizarin

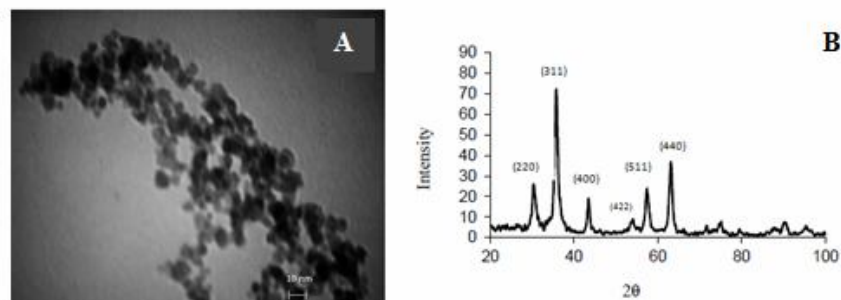


Fig. 1. (A) The TEM image of Fe_3O_4 nanoparticles. (B) XRD pattern of Fe_3O_4 nanoparticles.

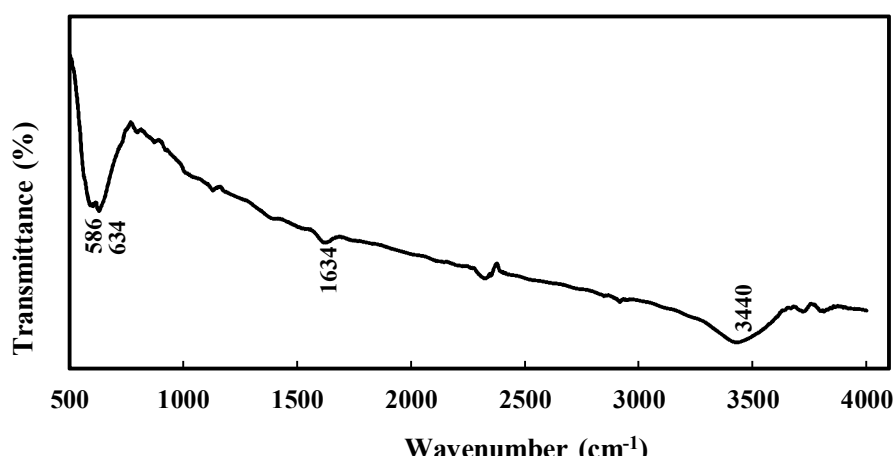


Fig. 2. FTIR spectra of Fe_3O_4 nanoparticles.

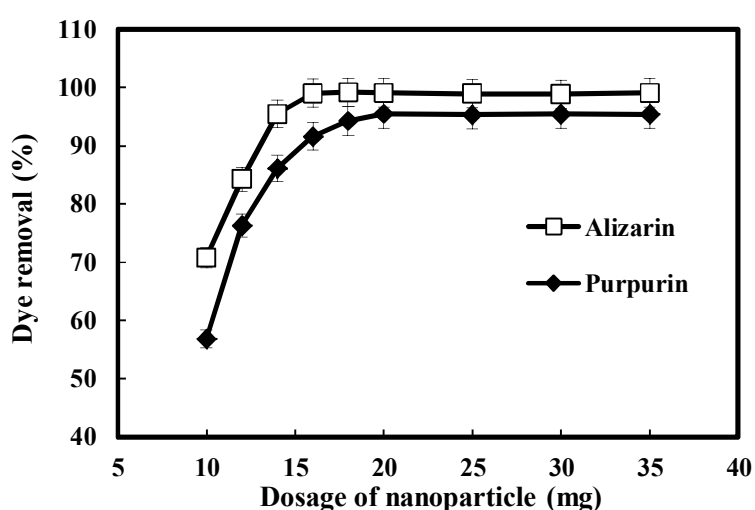


Fig. 3. FTIR spectra of alizarin (a), Fe_3O_4 nanoparticle (b), alizarin adsorbed Fe_3O_4 nanoparticle (c).

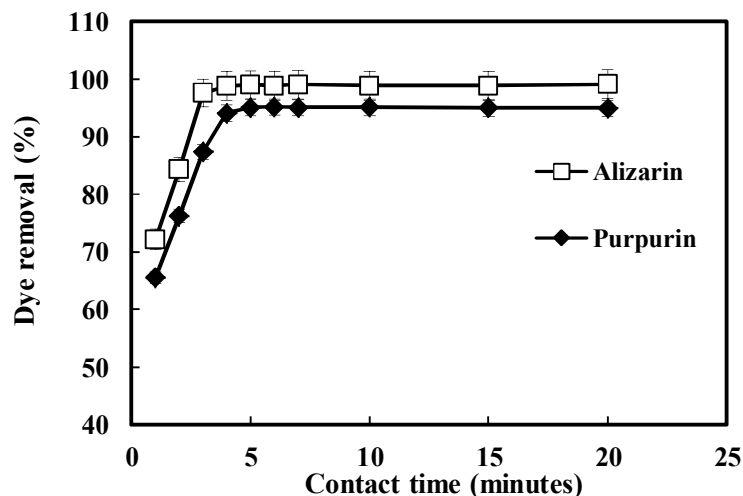


Fig. 4. FTIR spectra of Fe_3O_4 nanoparticle (a), purpurin (b), purpurin adsorbed Fe_3O_4 nanoparticle (c).

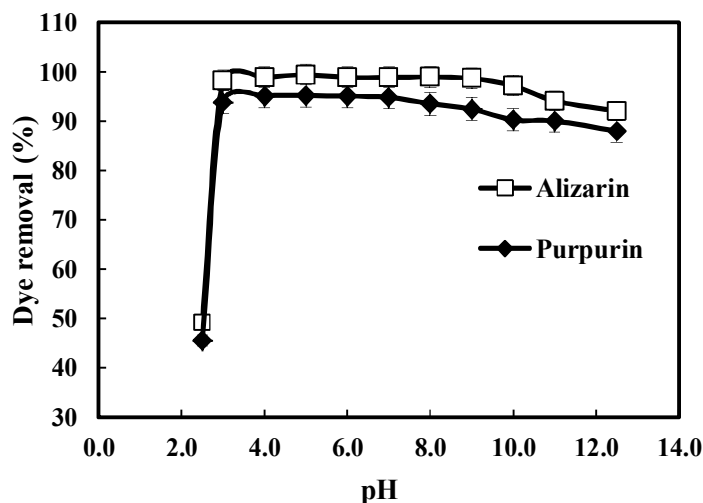


Fig. 5. Effect of dosage of Fe_3O_4 nanoparticles on removal of alizarin (□) and purpurin (◆); Experimental conditions: pH 5.0, initial dye concentration of 20.0 mg l^{-1} , stirring time of 5.0 min. The error bars correspond to the percentage of average deviations.

and purpurin from their individual aqueous solutions was found to be 20.0 mg .

The effect of the sample volume on the removal efficiency was investigated in the range of 10-100 ml. The results showed that using a sample volume in this range could not have a significant effect on the removal efficiency. This also indicates that the breakthrough volume must be higher than 100 ml.

Effect of Contact Time

The contact time between adsorbate and adsorbent is the most important design parameter affecting the performance of adsorption processes. The effect of contact time on the performance of Fe_3O_4 in adsorbing alizarin red and purpurin was investigated individually. The solution pH and Fe_3O_4 dosage were fixed at 5.0 and 20 mg, respectively. The initial dye concentrations for all test solutions were 20

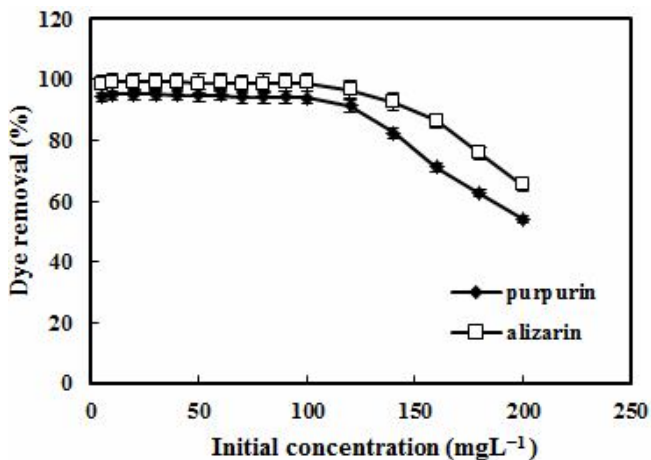


Fig. 6. Effect of stirring time on removal of alizarin (\square) and purpurin (\blacklozenge); Experimental conditions: Fe_3O_4 dosages of 20.0 mg, initial dyes concentrations of 20.0 mg l^{-1} and pH of 5.0. The error bars correspond to the percentage of average deviations.

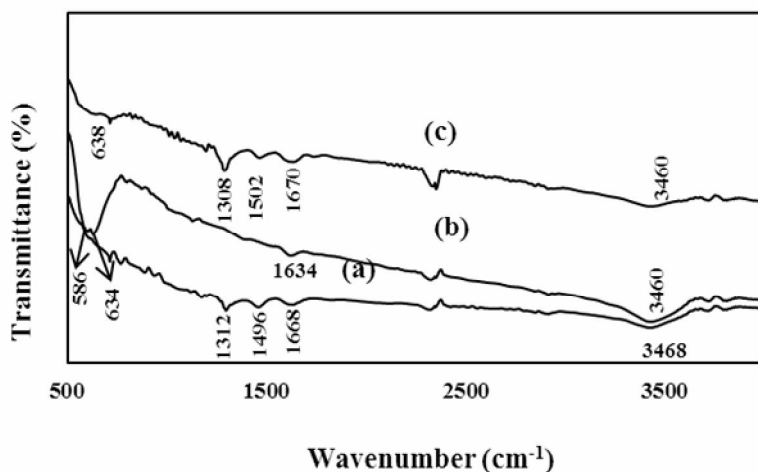


Fig. 7. Effect of initial pH of dye solution on removal of alizarin (\square) and purpurin (\blacklozenge); Experimental conditions: Fe_3O_4 dosage of 20.0 mg, initial dye concentration of 20.0 mg l^{-1} , stirring time of 5.0. The error bars correspond to the percentage of average deviations.

mg l^{-1} . Figure 6 shows the removal efficiencies for the two dyes as a function of stirring time in the range of 1.0-20.0 minutes. These data indicated that adsorption process started immediately upon adding Fe_3O_4 powder to both dye solutions. The removal efficiency for alizarin rapidly increased from 70%, in the first minute of contact, to a value of 99% when the stirring was continued to 5.0

min. For purpurin, the removal efficiency increased from 65.5%, in the first minute of contact, to 95% as the stirring was increased to 5.0 min where the equilibrium condition was attained. Therefore, the optimum contact time was considered to be 5.0 min for removal of both individual alizarin and purpurin sample solution. The contact time obtained in this study for equilibrium adsorption onto the

Fe_3O_4 nanoparticle is shorter than most of the literature reported values for dye adsorption by other adsorbents [12].

Effect of Solution pH

The pH of the dye solution plays an important role in the adsorption process because it can alter the surface properties of the adsorbent as well as the degree of ionization of the dyes. In this study, the influence of pH on adsorption of alizarin and purpurin onto the Fe_3O_4 surfaces was assessed for pHs of 2.5 to 12.5 and the results are shown in Fig. 7. The initial concentrations of dyes and adsorbent dosage were set at 20 mg l⁻¹ and 20 mg, respectively, with a stirring time of 5.0 min. Figure 7 shows that the removal of alizarin and purpurin is almost independent of pH and is almost quantitative at pHs higher than 3.0. This observation indicates that the adsorption of dyes on the surface of nanoparticles is independent of the electrical charges of either nanoparticles ($\text{pH}_{\text{pc}} = 6.5$) and dyes (for alizarin: $\text{pK}_{\text{a}1} = 5.25$ and $\text{pK}_{\text{a}2} = 11.5$; for purpurin: $\text{pK}_{\text{a}1} = 5.18$, $\text{pK}_{\text{a}2} = 7.65$ and $\text{pK}_{\text{a}3} = 10.27$). At pHs lower than 3.0, the decrease in dye removal could be due to dissolution of iron oxide nanoparticles [28]. Similar results for the effect of pH have been reported in the literature for the adsorption of these dyes onto the magnetite [29,30].

The adsorption capacity of Fe_3O_4 nanoparticles for dyes over the studied pH range could be an indication that the adsorption occurs by coordination of dye molecules with either Fe^{2+} or Fe^{3+} on the surface of nanoparticles. This has been reported in the literature regarding the textile dyeing by using alizarin which forms stable colored lake complexes with several metallic cations including Fe^{2+} and Fe^{3+} [30-33].

Effect of Dye Concentration

The initial dye concentration is another important variable that can affect on the adsorption process. Different concentrations of alizarin and purpurin were tested in order to find their adsorption amounts onto the surface of Fe_3O_4 nanoparticles under the previously determined optimum experimental conditions. The results, in terms of removal efficiency versus initial concentration of each dye, are shown in Fig. 8. According to this figure, the removal efficiency for alizarin was about 99% in the range of 5-100 mg l⁻¹ alizarin which decreased at its higher concentration

and reached to 65% at 200 mg l⁻¹. For purpurin, the removal efficiency was around 95% in the range of 5-100 mg l⁻¹ purpurin which decreased and finally reached to 55% at 200 mg l⁻¹. To follow the optimization procedure, 20 mg l⁻¹ for each dye was selected which not only quantitatively being adsorbed by the nanoparticles but also shorten the rate of the adsorption process. The results also indicates that Fe_3O_4 nanoparticles have shown approximately equal capacity for adsorption of both dyes. This is because alizarin red (240.20 g mol⁻¹) and purpurin (256.21 g mol⁻¹) have similar size and chemical structure as reported in Table 1.

Effect of Solution Ionic Strength

Most dye wastewaters contain salts, and the dyes adsorption was found to be strongly influenced by the concentration and nature of these ionic species [34,35]. Since the presence of any ion could affect on the hydrophobic and electrostatic interactions between dye and the surface of Fe_3O_4 nanoparticles as adsorbent, the effect of solution ionic strength on removal of alizarin and purpurin was investigated under the optimum experimental conditions in batch technique (Table 2). Selected concentrations of NaCl, in the range of 0.01-1.0 M, were added to individual beakers containing 10 ml of the tested dye solution (20 mg l⁻¹). The solution pH and Fe_3O_4 dosage were fixed at 5.0 and 20.0 mg, respectively, and the stirring time was 5.0 min. After the mixing time elapsed, the Fe_3O_4 nanoparticles were magnetically separated and the solution was analyzed for the residual dye. The results indicated that the adsorption capacities of Fe_3O_4 nanoparticles for alizarin and purpurin were not significantly affected with increasing NaCl concentration. This indicates that Na^+ and Cl^- ions do not compete with the positively- or negatively-charged groups of the dye molecules for being adsorbed onto the nanoparticles surface [24].

Effect of Solution Temperature

It is important to investigate the effect of temperature on adsorption in a view of practical application. The effect of temperature on the adsorption of alizarin and purpurin on Fe_3O_4 nanoparticles was investigated at an initial dye concentration of 20 mg l⁻¹. The solution pH and Fe_3O_4 dosage were fixed at 5.0 and 20.0 mg, respectively, and a stirring time of 5.0 min was used. Table 3 shows the

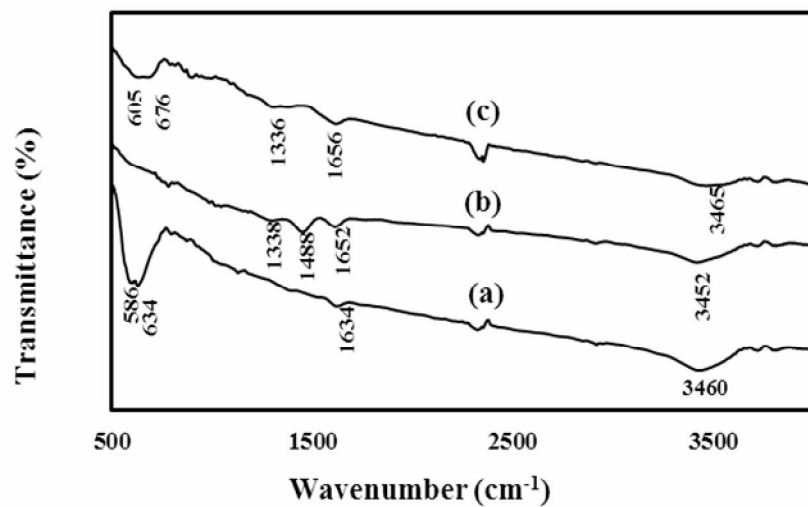


Fig. 8. Effect of initial dye concentration on removal of alizarin (□) and purpurin (◆); Experimental conditions: Fe_3O_4 dosage of 20.0 mg, pH 5.0, stirring time of 5.0 min. The error bars correspond to the percentage of average deviations.

Table 2. Effect of the Ionic Strength on Removal of Alizarin and Purpurin

NaCl (M)	Alizarin	Purpurin
0.00	99.78	95.54
0.02	99.84	95.56
0.04	99.82	95.50
0.06	99.68	95.20
0.08	99.72	95.48
0.10	99.72	95.45
0.20	99.70	95.48
0.40	99.67	95.32
0.60	99.80	95.20
0.80	99.75	94.84
1.00	99.65	95.50

Table 3. Effect of the Temperature on Removal of Alizarin and Purpurin

Temperature (K)	Alizarin	Purpurin
278	99.56	94.83
288	99.84	95.18
298	99.82	95.58
308	99.82	95.54
318	99.72	95.48

Table 4. Adsorption Isotherms Parameters of Alizarin and Purpurin onto Fe₃O₄ Nanoparticles

Dye	Langmuir			Freundlich		
	q _{max} (mg g ⁻¹)	b (L mg ⁻¹)	R ²	Log K _F (mg g ⁻¹)	n	R ²
Alizarin	45.87	0.50	0.999	1.34	4.94	0.972
Purpurin	40.48	0.94	0.997	0.71	2.56	0.964

Table 5. Adsorption Kinetic Constants of Alizarin and Purpurin onto Fe₃O₄ Nanoparticles

Dye	Pseudo-first-order model			Pseudo-second-order model		
	k ₁ (min ⁻¹)	q _e (mg g ⁻¹)	R ²	k ₂ (g mg ⁻¹ min ⁻¹)	q _e (mg g ⁻¹)	R ²
Alizarin	0.72	6.3	0.912	0.21	28.57	0.998
Purpurin	0.66	12.93	0.952	0.071	27.77	0.999

removal efficiencies for both dyes in a temperature range of 278-318 K. The results indicate that solution temperature has caused no significant variation in treatment efficiency of both dyes. This flexibility in working temperature represents an advantage over other methods [12], allowing

the treatment of several kinds of industrial effluents.

Adsorption Isotherms

Adsorption isotherms provide useful physicochemical data for better understanding and designing of a sorption

Table 6. Comparison of the Performance of the Present Adsorbent with some Reported in Literature

Adsorbent	Dye	Contact time	q_{\max} (mg g ⁻¹)	Ref.
Chitosan coating on the surface of magnetite (Fe_3O_4)	Alizarin red	50 min	40.12 mg g ⁻¹	[12]
$\text{Fe}_3\text{O}_4@\text{PPy}$ NPs ^a	Alizarin red-S	60 min	116.3 and 113.6 mg g ⁻¹	[41]
Au-NP-AC ^b	Alizarin yellow GG			
Activated carbon/ γ - Fe_2O_3 nano-composite	Alizarin Red S	5 min	123.4 mg g ⁻¹	[42]
Fe_3O_4	Alizarin red	5 min	45.87	This work

^aPolypyrrole coated magnetic nanoparticles. ^bGold nanoparticles loaded on activated carbon.

process as a unit operation. For this purpose, two well-known isotherm models, the Langmuir and Freundlich models, were applied for explanation of the adsorption data obtained in this study. The adsorption equilibrium data was applied to the Langmuir model described as follows [36]:

$$\frac{C_e}{q_e} = \frac{1}{bq_{\max}} + \frac{C_e}{q_{\max}} \quad (2)$$

where C_e shows the equilibrium concentration of dye (mg l⁻¹), and q_e is the amount of the dye adsorbed (mg) per gram onto the Fe_3O_4 nanoparticles. The q_{\max} is the surface concentration at monolayer coverage in mg g⁻¹ which indicates the maximum value of q_e that can be attained as C_e is increased. The b parameter is a coefficient related to the energy of adsorption and its value increases with increasing strength of the adsorption bond. Values of q_{\max} and b are determined from the linear regression plot of (C_e/q_e) vs. C_e . The adsorption equilibrium data were also applied to the Freundlich model [37]:

$$\log q_e = \log K_F + \frac{1}{n} \log C_e \quad (3)$$

where K_F and n are the constants from the Freundlich

equation representing the capacity of the adsorbent for the adsorbate and the reaction order, respectively. The reciprocal reaction order, $1/n$, is a function of the strength of adsorption. Table 4 summarizes the constants of models and their corresponding correlation coefficients. As shown in this table, R^2 of the Langmuir model is higher than that of the Freundlich isotherm for the adsorption of both investigated dyes, which means that the Langmuir sorption isotherm more accurately describes the sorptions of alizarin and purpurin onto the Fe_3O_4 nanoparticles. This in turn suggests that adsorption occurs as monolayer deposition of dyes. Also, as seen in this table, the maximum adsorption capacities for alizarin and purpurin on the Fe_3O_4 nanoparticles are 45.87 and 40.48 mg g⁻¹, respectively.

Adsorption Kinetic

To describe the adsorption behavior and rate, the data obtained from adsorption kinetic experiments were evaluated using pseudo-first- and pseudo-second-order reaction rate models. The pseudo-first-order Lagergren equation is given by [38]:

$$\log(q_e - q_t) = \log q_e - \frac{k_1 t}{2.303} \quad (4)$$

where k_1 is the pseudo-first-order rate constant (min^{-1}), q_e and q_t are the amount of dye adsorbed (mg g^{-1}) at equilibrium at time t (in min), respectively. The pseudo-second-order model can be expressed as [39]:

$$\frac{t}{q_t} = \frac{1}{k_2 q_e^2} + \frac{t}{q_e} \quad (5)$$

where k_2 ($\text{g mg}^{-1} \text{ min}^{-1}$) is the rate constant of pseudo-second-order adsorption. Kinetic constants obtained by linear regression for the two models are listed in Table 5. As shown in this table, higher values of R^2 were obtained for pseudo-second-order adsorption rate model indicating that the adsorption rates of both dyes onto the Fe_3O_4 nanoparticles can be more appropriately described by using the pseudo-second order rate. This means that the rate of the surface adsorption depends on the rate of the chemical adsorption process as the rate-determining step.

Desorption and Reusability Studies

For potential applications, the regeneration and reusability of an adsorbent are important factors to be reported. Possible desorption of alizarin and purpurin was tested by using 0.5 M NaOH solution as the eluent. The study revealed that the adsorbed alizarin and purpurin could be completely desorbed by NaOH solution. In this study, more than 95% of alizarin and 90% of purpurin was desorbed and recovered by 10 ml of NaOH solution when 10 ml of the dye with a concentration of 20 mg l^{-1} had been already adsorbed onto the Fe_3O_4 nanoparticles. The reusability of the adsorbents in several successive separation processes was tested and the result showed that the Fe_3O_4 nanoparticles can be recycled and reused for three times without significant reduction in their removal capacity.

CONCLUSIONS

In this study, Fe_3O_4 nanoparticles were produced and tested as adsorbents for the removal of alizarin and purpurin dyes from aqueous samples. The performed adsorption method by itself is not novel, however, it is novel in terms of materials employed; *i.e.* the Fe_3O_4 magnetic nanoparticles examined as possible adsorbents for the removal and separation of coexisting anthraquinone dyes (such as

alizarin and purpurin). The reusable Fe_3O_4 magnetic nanoparticles provided an efficient, fast, simple and inexpensive procedure for adsorption of alizarin and purpurin. The performance of Fe_3O_4 nanoparticles was comparable with other previously reported adsorbents, as shown in Table 6. High percentages of both dyes were removed from the sample by using Fe_3O_4 magnetic nanoparticles. As shown in Table 6, the time required for the separation of dyes on the surface of Fe_3O_4 was less than that for other adsorbents. Also, without modifying the adsorbent, that is a time-consuming process, we were able to easily remove these dyes from the aqueous sample.

The results indicated that the adsorbent shows higher capacity for removal of alizarin compared to purpurin, proving that the extra hydroxyl group in the para position in purpurin could be a reason for this observation as reported by other researchers. According to the structure of both dyes (Table 1), purpurin has an extra hydroxyl group in para position that increases the possibility of intermolecular H-bonding in this dye [40]. As a result, the interaction between the surface of the nanoparticles and purpurin reduces and the removal percentage of purpurin decreases.

The optimum dosage of nanoparticles and pH of the sample solution were obtained to be 20.0 mg and 5.0, respectively, while a stirring time of 5.0 min was applied for both dyes. The isotherm modeling revealed that the Langmuir equation could better describe the adsorption of both dyes onto the Fe_3O_4 nanoparticles as compared to Freundlich model. Kinetic data for both dyes were appropriately fitted to a pseudo-second-order adsorption rate. According to the results obtained in this research work, both alizarin and purpurin could be simply and inexpensively removed from aqueous solutions. However, the method could not selectively remove either purpurin or alizarin in the presence of each other. This could be achieved by modifying the surface of the nanoparticles with a purpurin- or alizarin-selective reagent that requires further research works.

ACKNOWLEDGEMENTS

The authors are grateful to Shiraz University Research Council for financial support of this project.

REFERENCES

- [1] Y. Anjaneyulu, N. Sreedhara Chary, D. Samuel Suman, *Environ. Sci. Technol.* 4 (2005) 245.
- [2] G. Sreelatha, P. Padmaja, *J. Envir. Protect. Sci.* 2 (2008) 63.
- [3] D. Bilba, D. Suteu, T. Malutan, *Cent. Eur. J. Chem.* 6 (2008) 258.
- [4] J.H. Weisburger, *Mutat. Res.* 506 (2002) 9.
- [5] H. Scheweppe, J. Winter, Madder and Alizarin, Artists Pigments, in: E. West Fitzhugh (Ed.), Oxford University Press, Oxford, 1997.
- [6] M. Panizza, M.A. Oturan, *Electrochim. Acta* 56 (2011) 7084.
- [7] C. Galindo, P. Jacques, A. Kalt, *Chemosphere* 45 (2001) 997.
- [8] C. Saez, M. Panizza, M.A. Rodrigo, G. Cerisola, *J. Chem. Technol. Biotechnol.* 82 (2007) 575.
- [9] A.M. Faouzi, B. Nasr, G. Abdellatif, *Dyes Pigm.* 73 (2007) 86.
- [10] F. Yi, S. Chen, *J. Por. Mater.* 15 (2008) 565.
- [11] M. Panizza, G. Cerisola, *Water Res.* 43 (2009) 339.
- [12] L. Fan, Y. Zhang, X. Li, Ch. Luo, F. Lu, H. Qiu, *Colloids Surf. B* 91(2012) 250.
- [13] M. Dabiri, Sh. Salimi, A. Ghassempour, A. Rassouli, M. Talebi, *J. Sep. Sci.* 28 (2005) 387.
- [14] V.K. Gupta, S. Khamparia; I. Tyagi, D. Jaspal, A. Malviya, A review, *Global J. Environ. Sci. Manage.* 1 (2015) 71.
- [15] D. Shao, G. Hou, J. Li, T. Wen, X. Ren, X. Wang, *Chem. Eng. J.* 255 (2014) 604.
- [16] Y. Huang, J. Li, X. Chen, X. Wang, *R. Soc. Chem. Adv.* 4 (2014) 62160.
- [17] S. Zhang, M. Zeng, W. Xu, J. Li, J. Li, J. Xu, X. Wang, *Dalton Trans.* 42 (2013) 7854.
- [18] M. Faraji, Y. Yamini, M. Rezaee, *J. Iran. Chem. Soc.* 7 (2010) 1.
- [19] G. Absalan, M. Asadi, S. Kamran, L. Sheikhan, D. M. Goltz, *J. Hazard. Mater.* 192 (2011) 476.
- [20] R. Manohar, V.S. Shrivastava, *J. Mater. Environ. Sci.* 6 (2015) 11.
- [21] W. Song, M. Liu, R. Hu, X. Tan, J. Li, *Chem. Eng. J.* 246 (2014) 268.
- [22] B. Saha, S. Das, J. Saikia, G. Das, *J. Phys. Chem. C* 115 (2011) 8024.
- [23] M. Safarikov, I. Safarik, *Eur. Cell. Mater.* 3 (2002) 192.
- [24] M. Ghaemi, G. Absalan, *J. Iran. Chem. Soc.* 12 (2015) 1.
- [25] M. Ghaemi, G. Absalan, L. Sheikhan, *J. Iran. Chem. Soc.* 11 (2014) 1759.
- [26] M.V. Canamares, J.V. Garcia-Ramos, C. Domingo, S. Sanchez-Cortes, *J. Raman Spectrosc.* 35 (2004) 921.
- [27] V.P. Glazunov, A.Y. Tchizhova, N.D. Pokhilo, V.Ph. Anufriev, G.B. Elyakov, *Tetrahedron* 58 (2002) 1751.
- [28] B. Zargar, H. Parham, A. Hatamie, *Talanta* 77 (2009) 1328.
- [29] S. Pirillo, Mari'a Luja'n Ferreira, H. Elsa, *Ind. Eng. Chem. Res.* 46 (2007) 8255.
- [30] S. Pirillo, Mari'a Luja'n Ferreira, H. Elsa, *J. Hazard. Mater.* 168 (2009) 168.
- [31] M.N. Bakola-Christianopoulou, *Polyhedron* 3 (1984) 729.
- [32] L.J. Larson, J.I. Zink, *Inorg. Chim. Acta* 169 (1990) 71.
- [33] S. Yariv, S. Shoval, *J. Chem.* 22 (1982) 259.
- [34] D.J. Greenland, *Soil Fert.* 28 (1965) 415.
- [35] M. Alkan, M. Dogan, *J. Colloid Interface Sci.* 243 (2001) 280.
- [36] I. Langmuir, *J. Am. Chem. Soc.* 40 (1918) 136.
- [37] H.M.F. Freundlich, *J. Phys. Chem.* 57 (1906) 385.
- [38] S. Lagergren, K. Svenska, *Vetensk.-Akad. Handl.* 24 (1898) 1.
- [39] Y.S. Ho, G. McKay, *Chem. Eng. J.* 70 (1998) 115.
- [40] L. Ford, Ch. M. Rayner, R.S. Blackburn, *Phytochemistry* 117 (2015) 168.
- [41] M. Ghavidel, Y. Yamini, M. Dayeni, Sh. Seidi, E. Tahmasebi, *J. Environ. Chem. Eng.* 3 (2015) 529.
- [42] M. Roosta, M. Ghaedi, M. Mohammadi, *Powder Technol.* 267 (2014) 134.
- [43] M. Fayazi, M. Ghanei-Motlagh, M.A. Taher, *Mater. Sci. Semicond. Process.* 40 (2015) 35.